1,2-Benzisothiazol-3-one 1,1-Dioxide Inhibitors of Human Mast Cell Tryptase

Keith D. Combrink,*,† H. Belgin Gülgeze,† Nicholas A. Meanwell,† Bradley C. Pearce,† Pi Zulan,‡ Gregory S. Bisacchi,‡ Daniel G. M. Roberts,§ Paul Stanley,▽ and Steven M. Seiler§

Department of Central Chemistry, Bristol-Myers Squibb Pharmaceutical Research Institute, Wallingford, Connecticut 06492-1927, Departments of Chemistry and Cardiovascular Biochemistry, Bristol-Myers Squibb Pharmaceutical Research Institute, P.O. Box 4000, Princeton, New Jersey 08543-4000, and Department of Dermatology, Bristol-Myers Squibb, 100 Forest Avenue, Buffalo, New York 14213-1032

Received August 6, 1998

A library of compounds were prepared by reacting 2-(bromomethyl)-1,2-benzisothiazol-3(2*H*)-one 1,1-dioxide (**5**) with commercially available carboxylic acids in the presence of potassium carbonate or a tertiary amine base. From this library, (1,1-dioxido-3-oxo-1,2-benzisothiazol-2(3*H*)-yl)methyl *N*-[(phenylmethoxy)carbonyl]-β-alanate (**7b**) emerged as a potent inhibitor of human mast cell tryptase ($IC_{50} = 0.85\ \mu M$). Extension of the side chain of **7b** by two carbons gave (1,1-dioxido-3-oxo-1,2-benzisothiazol-2(3*H*)-yl)methyl 5-[[(phenylmethoxy)carbonyl]amino]-pentanoate (**7d**) which was an 8-fold more potent inhibitor ($IC_{50} = 0.1\ \mu M$). Further modification of this series produced benzoic acid derivative (1,1-dioxido-3-oxo-1,2-benzisothiazol-2(3*H*)-yl)-methyl 4-[[(phenylmethoxy)carbonyl]amino]benzoate (**7n**) which is the most potent inhibitor identified in this series ($IC_{50} = 0.064\ \mu M$). These compounds exhibit time-dependent inhibition consistent with mechanism-based inhibition. For **7b**, the initial enzyme velocity is not a saturable function of the inhibitor concentration and the initial K_i could not be determined ($K_i > 10\ \mu M$). The steady-state rate constant, K_i^*, was determined to be 396 nM. On the other hand, compounds **7d** and **7n** are time-dependent inhibitors with a saturable initial complex. From these studies, an initial rate constant, K_i, for **7d** and **7n** was found to be 345 and 465 nM, respectively. The steady-state inhibition constants, K_i^*, for **7d** and **7n** were calculated to be 60 and 52 nM, respectively. Compound **7n** is a 13-fold more potent inhibitor than **7b,** and these kinetic studies indicate that the increase in inhibitory activity is due to an increase in initial affinity toward the enzyme and not an increase in chemical reactivity. These inhibitors generally show high selectivity for tryptase, being 40-fold weaker inhibitors of elastase, being 100-fold weaker against trypsin, and showing no inhibition against thrombin. These compounds are not inhibitors of thrombin, plasmin t-PA, urokinase, and factor Xa ($IC_{50} > 33\ \mu M$). In the delayed-type hypersensitivity (DTH) mouse model, a model of skin inflammation, a 5% solution of **7d** reduced edema by 69% compared to control animals.

Introduction

Human mast cell tryptase is a trypsin-like serine protease that can account for 20−25% of the total mast cell protein content and 95% of the trypsin-like activity in mast cells derived from lung and skin.[1] This protease is the major product secreted from these cells during mast cell activation. Elevated tryptase levels have been observed in a number of disease states such as asthma[2] and inflammatory skin diseases,[3] and tryptase may also function as a potent angiogenic factor.[4] Tryptase activity is not affected by endogenous serine protease inhibitors including α_2-macroglobin, α_1-proteinase inhibitor, aprotinin, and antithrombin. Although no endogenous inhibitors of human tryptase are known, tryptase activity appears to be regulated by dissociation of the tryptase tetramer which may involve heparin removal and competition for heparin between tryptase and heparin-binding proteins. A potent and selective inhibitor of tryptase will be an essential tool to determine the role of tryptase in inflammation and other processes. The tryptase tetramer is composed of four identical subunits, each containing an active site with trypsin-like specificity (cleaving adjacent to lysine or arginine residues).[5] The tetrameric structure is stabilized by heparin proteoglycans that are stored and secreted with the protease. Several human tryptase inhibitors, **1**−**4**, have been reported, and all contain one or more amidino or guanidino groups that direct the inhibitor to the P1 pocket to form a salt bridge with the aspartic acid residue at 189 in β-tryptase (chymotrypsinogen numbering used throughout). The second amidino or guanidino of **1**−**3** forms a salt bridge with a region of acidic residues remote from the active site.[5,6] Thus, the amidino or guanidino groups are essential structural features of the inhibitors **1** (BABCH),[7] **2** (BABIM),[8] and **3** (TPDCA).[6] One tryptase inhibitor, **4** (APC-366), is currently under clinical development for the treatment of asthma.[2,3] Some of these compounds have significant inhibitory activity against thrombin and trypsin which also have a P1 pocket that prefers basic amines.[9] However, the highly charged amidino or guanidino

† Department of Central Chemistry.
‡ Department of Chemistry.
§ Department of Cardiovascular Biochemistry.
▽ Department of Dermatology.

10.1021/jm9804580 CCC: $15.00
Published on Web 10/24/1998

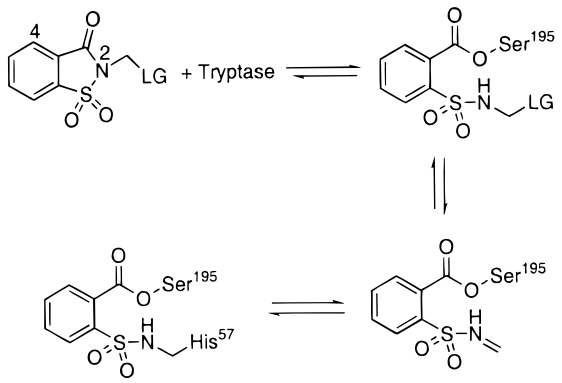

Figure 1. Proposed mechanism for the inhibition of tryptase.[11] For this figure chymotrypsinogen numbering is used for the active site serine and histidine.

groups in compounds **1**−**4** typically lead to poor oral bioavailability.

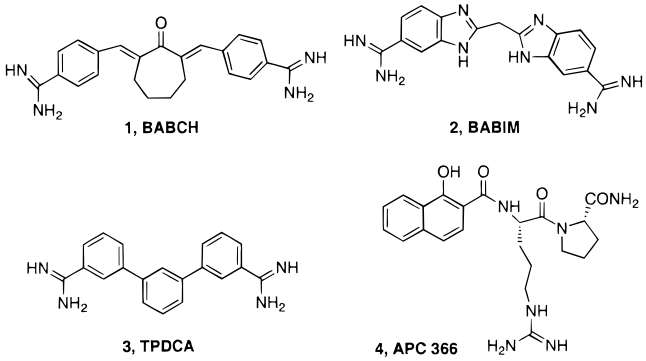

Benzisothiazolone 1,1-dioxide derivatives have been reported as mechanism-based inhibitors of the serine protease human leukocyte elastase (HLE).[10,11] Hlasta proposed, based on modeling studies of human leukocyte elastase, that substituents at the 4-position of the benzoisothiazolone interact with the S_1 specificity pocket of HLE while the 2-substituent (leaving group) projects into the S′ sites (Figure 1).[12] Traditional approaches to serine protease inhibition such as trifluoromethyl ketones, chloromethyl ketones, α-ketoesters, α-ketoamides, and α-ketoheterocycles generally rely upon optimization of interactions with the S_1−S_4 sites, and peptide-based inhibitors rarely project into the S′ sites.[13] However, recently several α-ketoheterocycle thrombin inhibitors that project functionality into the S_1′ region have been reported,[14] and Abeles has extended peptidomimetic inhibitors into the S′ direction with fluorinated α-keto acid derivatives,[15] demonstrating an important role for S′ site interactions. In this report, we describe the discovery and optimization of a series of benzisothiazolone 1,1-dioxide derivatives as inhibitors of human mast cell tryptase that rely predominantly upon interactions with S′ subsites of the enzyme for specificity and potency.[16] These compounds, notable by the absence of amidino or guanidino moieties, demonstrated efficacy in an animal model of inflammatory skin disease.

Chemistry

A diverse set of approximately 300 commercially available carboxylic acids were used to prepare a library of *N*-(acyloxy)benzisothiazolone 1,1-dioxide derivatives.

Scheme 1[a]

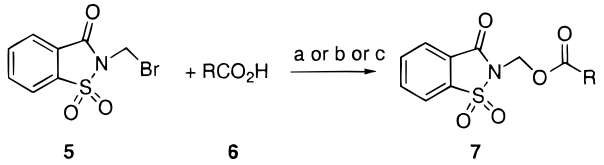

[a] (a) K_2CO_3, CH_3CN, Δ; (b) K_2CO_3, DMF; (c) DIEA, CH_3CN.

This library was prepared using parallel synthesis methods and automated purification when possible. The reaction of 2-(bromomethyl)-1,2-benzisothiazol-3(2*H*)-one (**5**) and the carboxylic acid **6** was carried out in CH_3CN at 60 °C in the presence of K_2CO_3 (2 equiv). The reactions were filtered and the polar impurities removed by passing the crude reaction mixture through a silica gel cartridge with CH_3CN as eluant. The compounds were analyzed by reverse-phase HPLC and MS. All compounds that had the correct predicted mass by mass spectral analysis and were at least 80% pure as judged by HPLC were evaluated for tryptase inhibitory activity.

This synthetic protocol was not useful for acids that were not soluble in CH_3CN. For these cases, the acid and base were stirred together in DMF at 23 °C and then treated with **5** (Scheme 1). The compounds were isolated by differential extraction and silica gel chromatography, if necessary. Acids not commercially available were prepared using literature methods. All active compounds were resynthesized, purified by silica gel chromatography, and characterized to appropriate standards.

Biochemistry

The benzisothiazolone 1,1-dioxide library was evaluated against a panel of viral and human proteases. Only our efforts to optimize the initial leads from this library as inhibitors of human skin tryptase will be described. Isolated human skin tryptase activity was measured in a 96-well microplate following cleavage of either 0.037 mM benzoylarginine *p*-nitroanilide (BAPNA) or 100 μM N-Cbz-Gly-Pro-Arg-pNA (similar data was obtained using either substrate). For routine compound evaluation, the fraction of control activity (FCA) was plotted as a function of the inhibitor concentration (I) and the curve was fit to $FCA/(1 + [I]/IC_{50})$ to determine the IC_{50}. The tryptase activity was measured in triplicate, and the average IC_{50} is reported in Table 1.

Results and Discussion

Individual compounds from the benzisothiazolone 1,1-dioxide library were evaluated for tryptase inhibitory activity with the result that compound **7b** was identified as the only submicromolar inhibitor. Consequently, **7b** was used as a starting point for further optimization of structure−activity relationships (SAR) for this series of human mast cell tryptase inhibitors. From these studies it was recognized that the distance between the benzisothiazolone 1,1-dioxide ring and the benzyloxycarbamate aromatic ring was important (Table 1). In the acyclic series **7a**−**l**, a series of linear carbon chain linkers were used and the four-carbon spacer is optimal as indicated by **7a**−**d** and **7i** (Table 1). Some substitution is tolerated in the acyclic linker with a preference for the *S* enantiomer as the L- and D-lysine derivatives,

Table 1. Inhibition of Human Mast Cell Tryptase by 1,2-Benzisothiazol-3-one 1,1-Dioxide Derivatives **7**

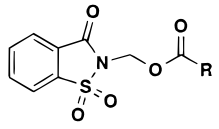

7

compd	method of preparation[a]	molecular formula[b]	mp (°C)	R	inhibn of human mast cell tryptase IC_{50} (μM) ± SD (no. of expts)
7a	A, B	$C_{18}H_{16}N_2O_7S$	oil	CH_2NH-Cbz	6.94 ± 1.56 (2)
7b	A, B	$C_{19}H_{18}N_2O_7S$	oil	CH_2CH_2NH-Cbz	0.854 ± 0.067 (4)
7c	A, B	$C_{20}H_{20}N_2O_7S$	oil	$(CH_2)_3$NHCbz	0.349 (1)
7d	A, B	$C_{21}H_{22}N_2O_7S\cdot 0.3$DMF	oil	$(CH_2)_4$NHCbz	0.11± 0.024 (3)
7e	A, B	$C_{21}H_{21}N_3O_8S$	oil	L-Ala-Gly-N-Cbz	13.4 ± 0 (2)
7f	A, B	$C_{20}H_{19}N_3O_8S\cdot H_2O$	oil	Gly-Gly-N-Cbz	0.9 ± 0.17 (3)
7g	A, B	$C_{26}H_{31}N_3O_9S$	oil	Nα-BOC-Nδ-Cbz-L-lysine	0.352 ± 0.078 (4)
7h	A, B	$C_{26}H_{31}N_3O_9S$	oil	Nα-BOC-Nδ-Cbz-D-lysine	12.2 ± 0.6 (3)
7i	A, B	$C_{22}H_{24}N_2O_7S$	oil	$(CH_2)_5$NHCbz	0.436 ± 0.031 (2)
7j	A, B	$C_{19}H_{26}N_2O_7S$	oil	$(CH_2)_5$NHBoc	5.37 ± 0.59 (2)
7k	A, B	$C_{21}H_{21}N_3O_8S$	oil	Gly-β-Ala-NCbz	0.255 ± 0.042 (6)
7l	A, B	$C_{22}H_{23}N_3O_8S$	oil	β-Ala-β-Ala-NCbz	>33 (3)
7m	B	$C_{23}H_{18}N_2O_7S$	127−128	C_6H_4-3-NHCbz	>33 (3)
7n	B	$C_{22}H_{18}N_2O_7S$	160−162	C_6H_4-4-NHCbz	0.0643 ± 0.0068 (7)
7o	B	$C_{24}H_{20}N_2O_6S$[c]	159−161	C_6H_4-4-NHCO$(CH_2)_2$Ph	0.17 ± 0.04 (3)
7p	B	$C_{24}H_{20}N_2O_6S\cdot 0.3H_2O$	oil	C_6H_4-4-CONH$(CH_2)_2$Ph	0.679 ± 0.083 (3)
7q	C	$C_{23}H_{19}N_3O_6S$	211−213	C_6H_4-4-CH_2NHCONHPh	0.157± 0.023 (3)
7r	C	$C_{23}H_{18}N_2O_7S$	67−68	C_6H_4-4-CH_2NCOOPh	0.63 ± 0.103 (3)
7s	B	$C_{23}H_{19}N_3O_6S\cdot 0.3H_2O$	171−173	C_6H_4-4-NHCONHCH_2Ph	0.95 ± 0.2 (3)
7t	B	$C_{23}H_{19}N_3O_6S$	189−190	C_6H_4-4-CH_2NHCOCH_2Ph	0.132 ± 0.013 (3)
7u	A, B	$C_{15}H_{12}N_2O_5S$	169−170	C_6H_4-4-NH_2	>33 (3)
7v	B	$C_{24}H_{20}N_2O_7S$	oil	C_6H_4-4-CH_2NHCOOCH_2Ph	0.352 ± 0.1 (3)
7w	B	$C_{23}H_{19}NO_7S$[d]	124−125	C_6H_4-4-O$(CH_2)_2$OPh	>33 (3)

[a] Method A, CH_3CN, K_2CO_3, 60 °C; method B, DMF, K_2CO_3, 23 °C; method C, DMF, Et$N(^iPr)_2$, 23 °C. [b] All compounds gave satisfactory combustion analysis unless noted. [c] C: calcd, 62.06; found, 60.98. HRMS: calcd, 465.1135; found, 465.1120. [d] C: calcd, 60.92; found, 59.24. H: calcd, 4.22; found, 3.65. HRMS: calcd, 454.09605; found, 454.09616.

7g and **7h,** respectively, show. Insertion of an additional amide group was detrimental to activity, even when the linker length was maintained at four atoms. The benzyloxycarbamate group is preferred over the *tert*-butoxycarbamate or simple alkyl groups. Compounds in which the terminal group was not an aromatic ring were not active. The most potent compound identified was the 4-[(carbobenzyloxy)amino]benzoic acid derivative **7n**. The carbamate carbonyl in this series of compounds is important for activity, but there is some flexibility as to the location of the carbonyl group. For example, derivitives **7o, 7q**, and **7t** are only 2.5-fold weaker than the most potent compound despite the variation of the location of the carbonyl moiety.

The benzisothiazolone 1,1-dioxide-based inhibitors of human mast cell tryptase inhibitors compiled in Table 1 are notable in that they lack a basic amidino or guanidino moiety that is a critical structural element of all inhibitors of this enzyme reported to date. Assuming a binding orientation as proposed for inhibition of HLE by benzisothiazolone 1,1-dioxide derivatives, the SAR summarized in Table 1 suggests that interactions between the inhibitor and the S′ region of tryptase are important for inhibitor recognition by the enzyme. Also, compounds **7a**−**w** are the first inhibitors of human mast cell tryptase that are derived from a mechanism-based chemotype, an aspect of biochemistry that was further examined by kinetic analysis of the mode of interaction of these compounds with the enzyme.

Kinetic Experiments. The benzisothiazolone 1,1-dioxide derivatives are time-dependent inhibitors of human mast cell tryptase consistent with their proposed mechanistic-based inhibitory activity. Inhibitors of this type can be divided into two general classes based on the relationship of the initial velocity with the inhibitor concentration.[17] With mechanism A (Figure 2), the initial affinity of the compound is low relative to the steady state. For this mechanism the initial enzyme velocity is independent of the inhibitor concentration. In mechanism B (Figure 2), the initial affinity of the compound for the enzyme is high enough to detect inhibition of the enzyme activity prior to reaching steady-state inhibition. For this mechanism the initial enzyme velocity is inhibited as a function of the inhibitor concentration.

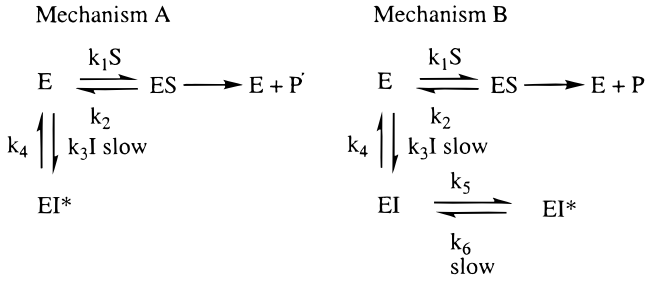

Figure 2. Two possible mechanisms of slow binding inhibitors.

The two mechanisms can also be differentiated kinetically by the rate of product formation as a function of time in the presence of varying concentrations of inhibitor. The results of these experiments, progress curves, are then fit to the integrated rate equation for slow binding inhibitors: $P = v_s t + (v_o - v_s)(1 - e^{-kt})/k$, where P is the concentration of *p*-nitroaniline product found and v_o, v_s, and k represent the initial enzyme velocity, steady-state velocity, and apparent first-order rate constant, respectively. The data were then fit to

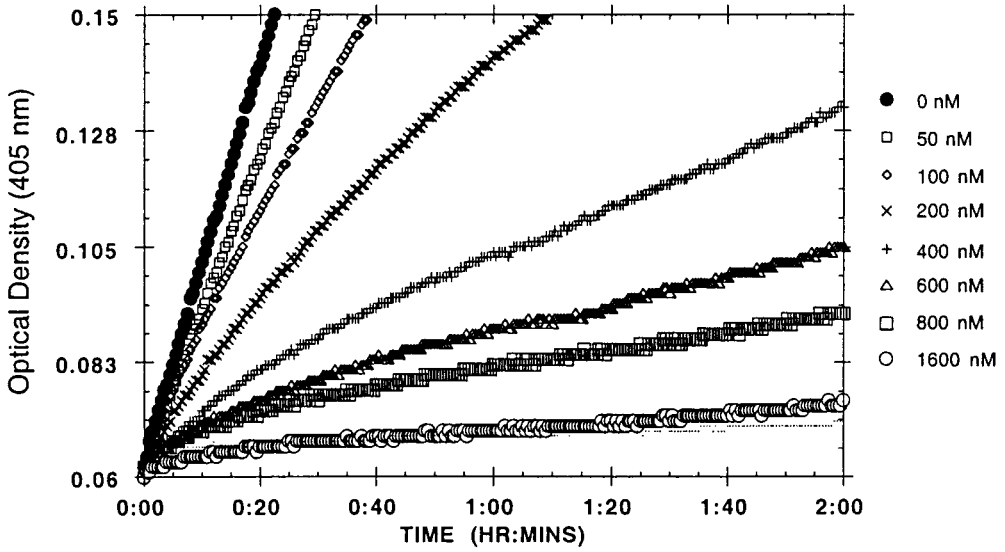

Figure 3. Progress curves showing the time-dependent inhibition of tryptase by the indicated concentrations of **7d**.

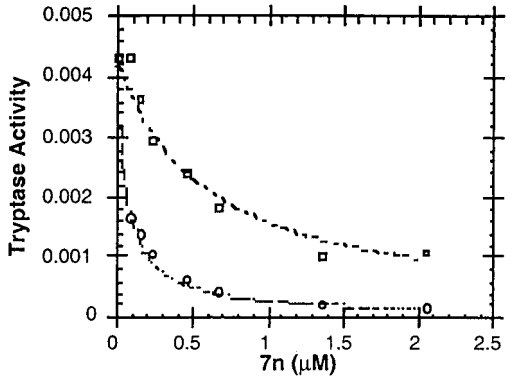

Figure 4. Plots of extracted data v_o (squares) and v_s (circles) to obtain K_i and K_i* values of 345 and 52 nM, respectively, for **7n**.

the above equation to determine v_o, v_s, and k. The initial enzyme velocity, v_o, was plotted as a function of inhibitor concentration, the data were fit to the equation: $v_o = v_{max}[S]/K_m(1 + [I]/K_i) + [S]$, and the initial inhibition constant K_i was obtained. In a similar manner, the steady-state velocity, v_s, was plotted as a function of inhibitor concentration, the data were fit to the equation: $v_s = v_{max}[S]/K_m(1 + [I]/K_i^*) + [S]$, and the steady-state inhibition rate constant K_i* was obtained. For **7b**, the initial enzyme velocity is not a saturable function of the inhibitor concentration and the initial rate constant K_i could not be determined ($K_i > 10\ \mu$M). The steady-state inhibition constant K_i* was determined to be 396 nM. On the other hand, compound **7d** is a time-dependent inhibitor with a saturable initial complex (Figure 3). From these studies an initial rate constant could be determined ($K_i = 345$ nM) and a steady-state inhibition constant $K_i^* = 60$ nM. Compound **7d** is a 8-fold more potent inhibitor than **7b**, and these kinetic studies indicate that the increase in activity is probably due to an increase in affinity toward the enzyme and not an increase in reactivity. A similar analysis for compound **7n** yields an initial rate constant, $K_i = 345$ nM, and a steady-state rate constant, $K_i^* = 52$ nM (Figure 4).

Specificity. Some of the more potent tryptase inhibitors were evaluated against a panel of other serine proteases, including HLE. These compounds were selective in that they were more potent inhibitors of tryptase than HLE and were not active against other serine proteases tested at concentrations up to 33 μM (Table 2). The most potent tryptase inhibitor, **7n**, was a 40-fold more potent inhibitor of this enzyme than HLE. Compounds **7b**, **7d**, and **7n** demonstrated weak inhibition of trypsin with a selectivity of 40−100-fold versus tryptase.

Tryptase Structure. Recently, the X-ray structure of human β-tryptase with 4-amidinophenylpyruvic acid (APPA) bound into the active site was reported.[18] Human β-tryptase is a tetramer arranged as a square flat ring with active sites directed toward an oval central pore which restricts the size of macromolecules that can be cleaved by tryptase.[18] The amidino group of APPA is bound to both carboxylate oxygens of Asp189 which occupies the bottom of the S_1 pocket. The phenyl ring of APPA is sandwiched between peptide planes 215−216 and 190−192.[18] The aromatic ring of the 1,2-benzisothiazol-3-one 1,1-dioxide derivatives could be accommodated in a similar manner. On the P′ side of the active site, side chains Tyr37B and Tyr74 of monomer A and Phe153 and the 152 spur of the neighboring monomer B limit substrate binding of extended substrate chains to P5′.[18] Thus, compounds **7i**−**l** are less active in the tryptase assay because the 2-substituent is too long to fit in the abbreviated P1′−P5′ sites of tryptase. The aromatic character of the P′ pocket bordered by Tyr37B and Tyr74 of monomer A and Phe153 of monomer B suggests that the preference for a terminal phenyl group in inhibitors **7** over simple alkyl groups could be due to a $\pi-\pi$ interaction between the terminal phenyl group in inhibitors **7** and the pocket bounded by Tyr37B and Tyr74 of monomer A and Phe153 of monomer B.

Animal Model. Tryptase is the major proteolytic protein in human mast cells and has been suggested to play a role in asthma and inflammatory skin disesases such as psoriasis[19] and atopic dermatitis.[20] To evaluate the effect of a tryptase inhibitor in a inflammatory disease model, compound **7d** was tested in a delayed-type hypersensitivity (DTH) mouse model of skin in-

Table 2. Inhibitory Activity of Benzisothiazolone 1,1-Dioxide Derivatives against a Panel of Proteases

compd	IC_{50} of human mast cell tryptase (μM) ± SD (no. of expts)	IC_{50} (μM) HLE	thrombin	trypsin	urokinase	plasmin	factor Xa
7b	0.854 ± 0.067(4)	2.26 ± 0.27	>33	33	>33	>33	>33
7d	0.11 ± 0.024(3)	1.44 ± 0.3	>33	>12	>33	33	>33
7n	0.0643 ± 0.0068(7)	2.66 ± 0.4	>33	NT	NT	NT	NT

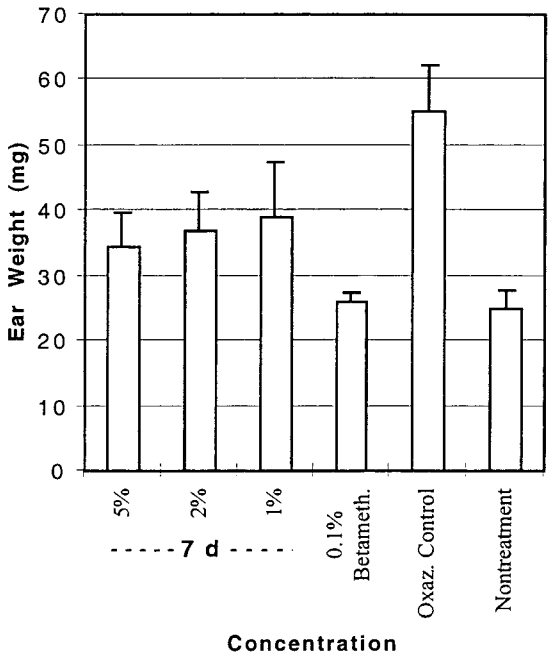

Figure 5. Effect of **7d** on edema in DTH mouse model. Data are expressed as the weight (mg) of an ear punch biopsy caused by inflammation.

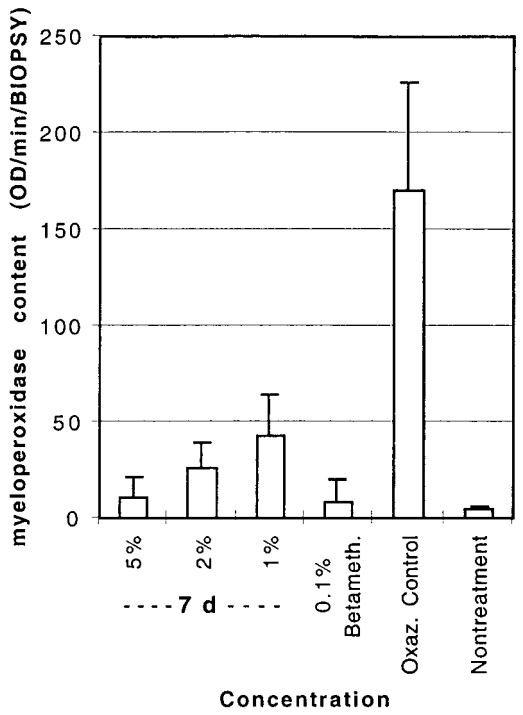

Figure 6. Effect of **7d** on neutrophil infiltration in the DTH mouse model as determined by the myeloperoxidase content (optical density/min/biopsy), an enzyme marker of PMN infiltration.

flammation.[21] Animals were sensitized to oxazolone on the first day and then challenged by application of oxazolone to the ear on the fifth day. In this experiment, the test agents were applied at the same time as oxazolone. A 5% solution of **7d** in acetone blocked the increase in ear weight due to edema by 69% compared to vehicle control (Figure 5). Compound **7d** also reduced myeloperoxidase content, an enzyme marker of polymorphonuclear leukocyte (PMN) infiltration, by 96% (Figure 6). By comparison, the steroid betamethasone dipropionate (0.1%) reduced edema by 96% and PMN infiltration by 98%. This is the first reported example of a tryptase inhibitor demonstrating efficacy in an animal model of inflammatory skin disease.

Conclusion

We have demonstrated that specifically functionalized benzisothiazolone 1,1-dioxide derivatives are potent and selective, mechanism-based inhibitors of human mast cell tryptase. These inhibitors are unique in that they lack a basic amidino or guanidino moiety that has been a critical structural feature of mast cell tryptase inhibitors reported thus far. Moreover, the benzisothiazolone 1,1-dioxide derivatives disclosed here are the first mechanism-based inhibitors of tryptase reported to date. The potency and selectivity of these compounds for mast cell tryptase in the absence of a conventional, basic P1 moiety probably result from the combination of chemically reactive functionality in the inhibitor that is directed into the active site by interactions with hydrophobic S′ regions unique to tryptase. Modeling studies suggest that these compounds recognize a hydrophobic binding pocket on the S′ side of tryptase that prefers a benzyloxycarbamate group approximately nine atoms from the electrophilic benzisothiazolone 1,1-dioxide carbonyl. One of these compounds, **7d**, has shown good activity in the delayed-type hypersensitivity (DTH) mouse model of skin inflammation, suggesting that a tryptase inhibitor may be effective in the treatment of inflammatory skin disorders.

Experimental Section

General Directions. Proton (^{1}H NMR) magnetic resonance spectra were recorded on either a Bruker AM or Varian Gemini FT instrument operating at 300 MHz. All spectra were recorded using residual solvent ($CHCl_3$ or DMSO) as internal standard. Signal multiplicity was designated according to the following abbreviations: s = singlet, d = doublet, m = multiplet, bs = broad singlet. IR spectra were obtained from Robertson Microlit of Madison, NJ, using a Perkin-Elmer system 2000 FTIR scanning from 4000 to 400 cm^{-1}. ESI-mass spectroscopy was performed via flow injection into a Finnigan SSQ 7000 quadrupole mass spectrometer in both positive and negative electrospray ionization (ESI) modes. Mobile phase: $CH_3CN/H_2O/NH_4OH$ (50/50/0.1). DCI-mass spectroscopy was performed via direct probe introduction into a Finnigan 4500 single quadrupole mass spectrometer in positive direct chemical ionization (DCI) mode with isobutane as reagent gas. Elemental analysis was provided by Robertson Microlit using a Perkin-Elmer model 2400 series 2 CHN elemental analyzer. Analytical HPLC was carried out using a YMC ODS column with gradient elution (10% MeOH/H_2O/0.2% H_3PO_4 to 90%

MeOH/H_2O/0.2% H_3PO_4) over 5 min and then a 3-min hold. 2-(Bromomethyl)-1,2-benzisothiazol-3(2*H*)-one 1,1-dioxide was prepared as previously described.[12] Acids **6a**−**l**, **6u**, and **6w** were purchased from commercial sources. Benzyl chloroformate, phenyl chloroformate, phenyl or benzyl isocyanate, or the appropriate acid chloride was used to prepare acids **6m**−**o**, **6s**, **6t**, or **6v** as previously described.[22−27]

4-[[[(Phenylamino)carbonyl]amino]methyl]benzoic Acid, 6q. A solution of 4-(aminomethyl)benzoic acid (1.00 g, 6.61 mmol) in 0.5 M NaOH (13 mL) was stirred at 0 °C, and PhNCO (1.1 mL, 10 mmol) was added. The mixture was stirred at 23 °C for 1 h and then stored at 0 °C for 48 h. H_2O was added and the mixture acidified with 2 N HCl to pH = 2. The solution was filtered and the solid recrystallized from MeOH/H_2O to give 1.71 g (96%) of **6q** as a white solid: mp 165−168 °C; ^{1}H NMR (DMSO-d_6) δ 4.36 (d, J = 6.0 Hz, 2H), 6.78 (t, J = 6.0 Hz, 1H), 6.89−6.97 (m, 2H), 7.15−7.29 (m, 2H), 7.38−7.48 (m, 3H), 7.90 (d, J = 8.2 Hz, 2H), 8.71 (s, 1H, exchanges with D_2O), 9.00 (s, 1H, exchanges with D_2O); IR (KBr) 1692, 1633, 1558 cm^{-1}; MS *m*/*z* 269 (M^-). Anal. Calcd for $C_{15}H_{14}N_2O_3 \cdot 0.12H_2O$: C, 66.13; H, 5.27; N, 10.67. Found: C, 65.75; H, 5.37; N, 10.67.

4-[[(Phenoxycarbonyl)amino]methyl]benzoic Acid, 6r. A solution of 4-(aminomethyl)benzoic acid (0.96 mg, 6.3 mmol) in dioxane (10 mL) and 10% $NaHCO_3$ (20 mL) was cooled to 0 °C, treated with a solution of phenyl chloroformate (0.80 mL, 6.3 mmol), warmed to room temperature, and stirred for 12 h. The solvent was removed, and H_2O was added. The solution was acidified to pH 1−2 and filtered and the solid purified by flash chromatography using 10% MeOH/$CHCl_3$ as eluant to give 0.70 g (40%) of **6r** as a white solid. The solid was recrystallized from MeOH/H_2O to give white needles: mp 167−170 °C; ^{1}H NMR (DMSO-d_6) δ 4.36 (d, J = 5.8 Hz, 2H), 6.82−6.97 (m, 1H), 7.19−7.29 (m, 2H), 7.37−7.43 (m, 2H), 7.50 (d, J = 7.7 Hz, 2H), 7.92 (d, J = 7.7 Hz, 2H), 8.76 (s, 1H, exchanges with D_2O), 9.33 (s, 1H, exchanges with D_2O); IR (KBr) 1706, 1542 cm^{-1}; MS *m*/*z* 270 (M^-). Anal. Calcd for $C_{15}H_{13}NO_4 \cdot 3.4H_2O$: C, 54.18; H, 6.00; N, 4.21. Found: C, 54.19; H, 5.79; N, 4.06.

Method A. A mixture of acid (0.2 mmol) and K_2CO_3 (0.25 mmol) in CH_3CN (2 mL) was treated with a solution of 2-(bromomethyl)-1,2-benzisothiazol-3(2*H*)-one 1,1-dioxide (0.18 mmol) in CH_3CN (2 mL). The mixture was heated to 60 °C for 2 h, cooled, filtered through a silica gel (2 g) cartridge, and washed with 10 mL of CH_3CN. A sample of the filtered solution was analyzed by ESI-MS and HPLC (major peak ≥ 80%). Compounds using commercially available acids were intially prepared by method A in parallel solution-phase reactions.

Method B. A solution of acid (14.7 mmol) in DMF (30 mL) was treated with K_2CO_3 (7.0 mmol) followed by 2-(bromomethyl)-1,2-benzisothiazol-3(2*H*)-one 1,1-dioxide (1.19 g, 4.3 mmol) and stirred for 12 h at 23 °C. The mixture was diluted with EtOAc, extracted with H_2O and saturated NaCl(aq), dried ($MgSO_4$), and concentrated. The residue was chromatographed on silica gel with EtOAc in hexanes as eluant to give product.

Method C. A mixture of 2-(bromomethyl)-1,2-benzisothiazol-3(2*H*)-one (221 mg, 0.8 mmol), diisopropylethylamine, and acid (227 mg, 0.84 mmol) in CH_3CN (10 mL) was stirred for 12 h at room temperature. The solvent was removed and the solid triturated with MeOH and isolated by filtration.

(1,1-Dioxido-3-oxo-1,2-benzisothiazol-2(3*H*)-yl)methyl 4-aminobenzoate, **7u,** was prepared with 4-aminobenzoic acid using method B to give **7u** (41%), and the following spectral data were obtained: ^{1}H NMR (DMSO-d_6) δ 5.93 (s, 2H), 6.11 (s, 2H, exchanges with D_2O), 6.54 (d, J = 6.9 Hz, 2H), 7.61 (d, J = 6.9 Hz, 2H), 7.99−8.15 (m, 2H), 8.17 (d, J = 6.9 Hz, 1H), 8.34 (d, J = 6.9 Hz, 1H); IR (KBr) 3380, 3455, 1735, 1705, 1355, 1169, 1199 cm^{-1}; MS *m*/*z* 332 (MH^+). Anal. Calcd for $C_{15}H_{12}N_2O_5S$: C, 54.21; H, 3.64; N, 8.43; S, 9.65. Found: C, 53.91; H, 3.76; N, 8.30; S, 9.35.

Biological Evaluation. 1. Tryptase Assay. Human skin tryptase (purchased from Dr. Norman Schechter, Department of Dermatology, University of Pennsylvania Medical Center, Philadelphia, PA) was diluted in 2 M NaCl, 10 mM MOPS, pH 6.8, to give a working stock solution of approximately 165 nM. The substrate, benzoylarginine *p*-nitroaniline (BAPNA), was prepared as a 10 mM stock solution in 90% DMSO. Low-molecular-weight heparin (Calbiochem 375097) was prepared as a 5 mg/mL stock solution in H_2O. Assay buffer was prepared by combining 1.1 mL of the 5 mg/mL heparin stock solution, 5.5 mL of 2 M NaCl, 0.9 M Tris (HCl), pH 8.0, and 43 mL of H_2O. The compound to be tested was prepared initially as a 10 mM stock solution in DMSO.

To each well of a 96-well microplate (Nunc MaxiSorp), 250 μL of assay buffer was pipetted followed by 2.0 μL of the test compound in DMSO; 10 μL of the substrate was then added to give a final concentration of either 0.37 mM BAPNA or 100 μM N-Cbz-Gly-ProArg-pNA (similar data was obtained using either substrate). The microplate was then shaken on a platform vortex mixer at a setting of 800 (Sarstedt TPM-2); 10 μL of the 165 nM working stock solution of human skin tryptase was then added to each well (6 nM final concentration). The microplate was again vortexed at a setting of 800 for 1 min, and the incubation of the sample was continued without shaking for an additional 2 min. The microplate was read on a microplate reader (Molecular Devices UV max) at room temperature in the kinetic mode over 20 min at 405 nm.

The (1,1-dioxido-3-oxo-1,2-benzisothiazol-2(3*H*)-yl)methyl ester inhibitors showed no detectable degradation at pH 8.0 (TRIS/HCl buffer) after 1 h at room temperature as judged by reverse-phase HPLC analysis (UV at either 220 or 254 nm).

HLE was also measured following the cleavage of the *p*-nitroanilide substrate in microtiter plate format. The enzymatic assays were performed with 9.5 nM HLE and 100 μM methoxysuccinyl-Ala-Ala-Pro-Val-pNA substrate (K_m = 43.6 μM).

Enzymatic activity of human α-thrombin (Sigma) was measured in a buffer containing 0.145 M NaCl, 0.005 M KCl, 1 mg/mL poly(ethylene glycol) (PEG-8000), 0.030 M HEPES (pH 7.4), and 0.03 U/mL final thrombin concentration using a microtiter plate-based assay. The enzyme was incubated at room temperature with the inhibitor for 3 min prior to starting the reaction with 10 mM S-2238 (D-Phe-Pip-Arg-pNA; K_m = 2.54 μM).

Plasmin (Kabi Vitrum) was measured as for thrombin except that the buffer was 50 mM TRIS/Cl (pH 7.8) and the reaction was initiated with 100 μM S-2251 (D-Val-Leu-Lys-pNA; K_m = 98 μM). Recombinant tissue plasminogen activator (Genentech), human factor Xa (Kabi Vitrum), and urokinase (Abbott Labs, Abbokinase) were assayed in the same buffer as thrombin, but the reactions were started with 100 μM Spectrozyme t-PA (methylsulfonyl-D-cyclohexyltyrosyl-Gly-Arg-pNA; K_m = 90 μM), 100 μM S-2222 (phenyl-Ile-Glu-Gly-Arg-pNA; K_m = 87 μM), and 100 μM S-2444 (L-pyroGlu-Gly-Arg-pNA), respectively. Bovine pancreatic trypsin (Sigma) was assayed in 2 mM $CaCl_2$, 50 mM TRIS/Cl (pH 8.0), and the reaction was started with 100 μM Chromozym-TRY (carboxybenzoxy-Val-Gly-Arg-pNA; K_m = 46 μM).

2. Delayed-Type Hypersensitivity Assay in Mice. Groups of 8 swiss mice (female, Charles River) weighing 20−25 g were sensitized to the sensitizing agent oxazolone in the following manner: On day 0 an induction dose of 25 μL of oxazolone in acetone was applied to the shaved ventral region of each animal. On day 4, a sensitizing dose of 20 μL of 0.5% oxazolone in acetone was applied to the inner and outer surface of each ear (10 μL/surface) together with the test compound (co-applied). Appropriate control groups of animals were included.

Twenty-four hours later, the inflammatory response was evaluated. A punch biopsy ($^5/_{16}$ in., 15−30 mg) of each ear was removed from the euthanized animals and weighed. The weight increase caused by the inflammation is a measure of edema which is used to assess the effect of test compounds. The same punch biopsies were then frozen in liquid nitrogen for later analysis of the myeloperoxidase content, an enzyme marker of PMN infiltration into the inflamed tissue.[28]

Acknowledgment. We thank Dr. William Kreighbaum for assistance with nomenclature and Dr. Malcolm Davis, Computer Aided Drug Design, Bristol-Myers Squibb, Princeton, NJ, for evaluation of several of these compounds in a homology model of a monomer of human mast cell tryptase.

References

(1) Schwartz, L. B. In *Neutral Proteases of Mast Cells*; Schwartz, L. B., Ed.; Karger: Basel, 1990; Vol. 27, pp 90−113.
(2) Clark, J. M.; Abraham, W. M.; Fishman, C. E.; Forteza, R.; Ahmed, A.; Cortes, A.; Warne, R. L.; Moore, W. R.; Tanaka, R. D. Tryptase Inhibitors Block Allergen-induced Airway and Inflammatory Responses in Allergic Sheep. *Am. J. Respir. Crit. Care Med.* **1995**, *152*, 2076−2083.
(3) Clark, J. M.; Moore, W. R.; Tanaka, R. D. Tryptase Inhibitors: A New Class of Antiinflammatory Drugs. *Drugs Future* **1996**, *21*, 811−816.
(4) Blair, R. J.; Meng, H.; Marchese, M. J.; Ren, S.; Schwartz, L. B.; Tonnesen, M. G.; Gruber, B. L. Human Mast Cells Stimulate Vascular Tube Formation: Tryptase is a Novel, Potent Angiogenic Factor. *J. Clin. Invest.* **1997**, *99*, 2691−2700.
(5) Johnson, D. A.; Barton, G. J. Mast cell tryptase: Examination of Unusual Characteristics by Multiple Sequence Alignment and Molecular Modeling. *Protein Sci.* **1992**, *1*, 370−377.
(6) Stubbs, M. T.; Morenweiser, R.; Sturzebecher, J.; Bauer, M.; Bode, W.; Huber, R.; Piechottka, G. P.; Matschiner, G.; Sommerhoff, C. P.; Fritz, H.; Auerswald, E. A. The Three-Dimensional Structure of Recombinant Leech-derived Tryptase Inhibitor in Complex with Trypsin − Implications for the Structure of Human Mast Cell Tryptase and its Inhibition. *J. Biol. Chem.* **1997**, *272*, 19931−19937.
(7) Stürzebecher, J.; Prasa, D.; Sommerhoff, C. P. Inhibition of Human Mast Cell Tryptase by Benzamidine Derivatives. *Biol. Chem. Hoppe-Seyler* **1992**, *373*, 1025−1030.
(8) Caughey, G. H.; Raymond, W. W.; Bacci, E.; Lombardy, R. J.; Tidwell, R. R. Bis(5-amidino-2-Benzimidazolyl)Methane and Related Amidines Are Potent, Reversible Inhibitors of Mast Cell Tryptases. *J. Pharmacol. Exp. Ther.* **1993**, *264*, 676−682.
(9) Han, W. T.; Trehan, A. K.; Wright, J. J. K.; Frederici, M. E.; Seiler, S. M.; Meanwell, N. A. Azetidin-2-one Derivatives as Inhibitors of Thrombin. *Bioorg. Med. Chem.* **1995**, *3*, 1123−1143.
(10) Groutas, W. C.; Brubaker, M. J.; Venkataraman, R.; Epp, J. B.; Houser-Archield, N.; Chong, L. S.; McClenahan, J. J. Potential Mechanism-Based Inhibitors of Proteolytic Enzymes. *Bioorg. Med. Chem. Lett.* **1992**, *2*, 175−180.
(11) Hlasta, D. J.; Bell, M. R.; Boaz, N. W.; Court, J. J.; Desai, R. C.; Franke, C. A.; Mura, A. J.; Subramanyam, C.; Dunlap, R. A Benzisothiaolone Class of Potent, Selective Mechanism-Based Inhibitors of Human Leukocyte Elastase. *Bioorg. Med. Chem. Lett.* **1994**, *4*, 1801−1806.
(12) Hlasta, D. J.; Bell, M. R.; Court, J. J.; Cundy, K. C.; Desai, R. C.; Ferguson, E. W.; Gordon, R. J.; Kumar, V.; Maycock, A. L.; Subramanyam, C. The Design of Potent and Stable Benzisothiazolone Inhibitors of Human Leukocyte Elastase. *Bioorg. Med. Chem. Lett.* **1995**, *5*, 331−336.
(13) Edwards, P. D.; Bernstein, P. R. Synthetic Inhibitors of Elastase. *Med. Res. Rev.* **1994**, *14*, 127−194.
(14) Costanzo, M. J.; Maryanoff, B. E.; Hecker, L. R.; Schott, M. R.; Yabut, S. C.; Zhang, H.; Andrade-Gordon, P.; Kauffman, J. A.; Lewis, J. M.; Krishnan, R.; Tulinsky, A. Potent Thrombin Inhibitors that Probe the S_1' Subsite: Tripeptide Transition State Analogues Based on a Heterocycle-Activated Carbonyl Group. *J. Med. Chem.* **1996**, *39*, 3039−3043.
(15) Abeles, R. H.; Parisi, M. F. Inhibition of Chymotrypsin by Fluorinated α-Keto Acid Derivatives. *Biochemistry* **1992**, *31*, 9429−9435.
(16) Shortly after this work was completed, Groutas reported a series of amino acid-derived phthalimide and benzisothiazolone inhibitors of HLE and proteinase 3: Groutas, W. C.; Chong, L. S.; Venkataraman, R.; Kuang, R.; Epp, J. B.; Houser-Archield, N.; Huang, H.; Hoidal, J. R. Amino Acid-Derived Phthalimide and Saccharin Derivatives as Inhibitors of Human Leukocyte Elastase, Cathepsin G and Proteinase 3. *Arch. Biochem. Biophys.* **1996**, *332*, 335−340.
(17) Morrison, J. F. The Slow-binding and Slow, Tight-binding Inhibition of Enzyme-catalysed Reactions. *Trends Biochem. Sci.* **1982**, *7*, 102−105.
(18) Pereira, P. J. B.; Bergner, A.; Macedo-Ribeiro, S.; Huber, R.; Matschiner, G.; Fritz, H.; Sommerhoff, C. P.; Bode, W. Human β-Tryptase is a Ring-like Tetramer with Active Sites Facing a Central Pore. *Nature* **1998**, *392*, 306−311.
(19) Michaelsson, G.; Kraaz, W.; Hagforsen, E.; Pihl-Lundin, I.; Lööf, L. Psoriasis Patients Have Highly Increased Numbers of Tryptase-positive Mast Cells in the Duodenal Stroma. *Br. J. Dermatol.* **1997**, *136*, 866−870.
(20) Järvikallio, A.; Naukkarinen, A.; Harvima, I. T.; Aalto, M. L.; Horsmanheimo, M. Quantitative Analysis of Tryptase- and Chymase-containing Mast Cells in Atopic Dermatitis and Nummular Eczema. *Br. J. Dermatol.* **1997**, *136*, 871−877.
(21) Garrigue, J. L.; Nicolas, J. F.; Demidem, A.; Bour, H.; Viac, J.; Thivolet, J.; Schmitt, D. Contact Sensitivity in Mice: Differential Effect of Vitamin D3 Derivative (calcipotriol) and Corticosteroids. *Clin. Immunol. Immunopathol.* **1993**, *67*, 137−42.
(22) Leone-Bay, A.; Ho, K.-K.; Agarwal, R.; Baughman, R. A.; Chaudhary, K.; DeMorin, F.; Genoble, L.; McInnes, C.; Lercara, C.; Milstein, S.; O'Toole, D.; Sarubbi, D.; Variano, B.; Paton, D. R. 4-[4-[(2-Hydroxybenzoyl)amino]phenyl]butyric Acid as a Novel Oral Delivery Agent for Recombinant Human Growth Hormone. *J. Med. Chem.* **1996**, *39*, 2571−2578.
(23) Krzyzanowski, L.; Rzeszotarska, B. Synthesis of *N*-(p-Carbobenzoxyaminobenzoyl)-L-Glutamic Acid α-Benzyl Ester. *Org. Prep. Proced. Int.* **1985**, *17*, 83−89.
(24) Ryan, T. J.; Fenton, J. W.; Chang, T.-L.; Feinman, R. D. Specificity of Thrombin: Evidence for Selectivity in Acylation Rather Than Binding for *p*-Nitrophenyl α-Amino-*p*-toluate. *Biochemistry* **1976**, *15*, 1337−1341.
(25) Dixon, J.; Ince, F.; Tinker, A. C. Phenylethylamines and Compositions Containing Them. EP 142283 A2; Fisons PLC: U.K., 1985; p 120.
(26) Rafferty, M. F.; Johnson, G. Preparation of Benzoic Acid and Benzoic Acid Ester Derivatives Having Antiinflammatory and Analgesic Activity. EP 226223 A2; Warner-Lambert Co.; 1987; p 27.
(27) Conn, M. M.; Deslongchamps, G.; de Mendoza, J.; Rebek, J., Jr. Convergent Functional Groups. 13. High-affinity Complexation of Adenosine Derivatives within Induced Binding Pockets. *J. Am. Chem. Soc.* **1993**, *115*, 3548−3557.
(28) Bradley, P. P.; Priebat, D. A.; Christensen, R. D.; Rothstein, G. Measurement of Cutaneous Inflammation: Estimation of Neutrophil Content with an Enzyme Marker. *J. Invest. Dermatol.* **1982**, *78*, 206−209.

JM9804580